

See discussions, stats, and author profiles for this publication at: <https://www.researchgate.net/publication/235770900>

Theoretical Design of the Molecular Structure of Bent-Core Mesogens with Large Second-Order Nonlinear Optical Properties

ARTICLE *in* THE JOURNAL OF PHYSICAL CHEMISTRY C · APRIL 2012

Impact Factor: 4.77 · DOI: 10.1021/jp300072k

CITATIONS

12

READS

16

4 AUTHORS, INCLUDING:



Benoît Champagne

University of Namur

401 PUBLICATIONS 8,708 CITATIONS

SEE PROFILE



Julien Guthmuller

Gdansk University of Technology

48 PUBLICATIONS 623 CITATIONS

SEE PROFILE



Armand Soldera

Université de Sherbrooke

95 PUBLICATIONS 895 CITATIONS

SEE PROFILE

Theoretical Design of the Molecular Structure of Bent-Core Mesogens with Large Second-Order Nonlinear Optical Properties.

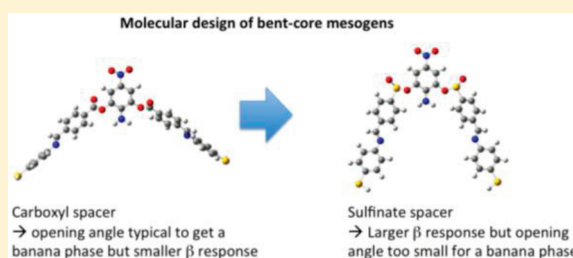
Benoît Champagne,^{*,†} Julien Guthmuller,[‡] Frédéric Perreault,[§] and Armand Soldera^{*,§}

[†]Laboratoire de Chimie Théorique, Unité de Chimie Physique Théorique et Structurale, Facultés Universitaires Notre-Dame de la Paix (FUNDP), rue de Bruxelles, 61, B-5000 Namur, Belgium

[‡]Faculty of Applied Physics and Mathematics, Gdansk University of Technology, Narutowicza 11/12, 80233, Gdansk, Poland

[§]Centre Québécois des Matériaux Fonctionnels, Département de Chimie, Université de Sherbrooke, Sherbrooke, Québec, Canada J1K 2R1

ABSTRACT: The first hyperpolarizability of two series of molecules with bent-shaped structures has been calculated at the ab initio level. The two series consist of carboxyl derivatives for which some molecules are known to exhibit banana phases and of their sulfinate homologues that have not been synthesized yet. The final purpose is to reveal the relevance or not in synthesizing these latter molecules. The strategy is based on reporting the effect of the positions of donor and acceptor groups on the central benzene ring on the structural parameters and on the first hyperpolarizabilities. It is shown that in the sulfinate series the larger first hyperpolarizabilities are incompatible with efficient geometrical character while for the carboxyl series, the opening angle between the molecular arms is typical of banana-shaped molecules but the first hyperpolarizability is only slightly enhanced. Calculations thus reveal that the sulfinate series does not need to be synthesized, whereas they show that our approach can be naturally applied to the development of new bent-shaped molecules for nonlinear optical applications.



I. INTRODUCTION

Bent-core liquid crystals (LC), also known as banana-shaped liquid crystals, constitute interesting systems with remarkable properties.¹ Indeed, it was demonstrated in 1996 that molecules incorporating a bent-shaped rigid core, i.e., bent-core mesogens, show polar order and chiral superstructures in their LC phases despite the fact that constituent molecules are not chiral.² Owing to polar order, the mesophases can give rise to ferroelectric switching, whereas their intrinsic noncentrosymmetry make them compatible with second-order nonlinear optical (NLO) processes. The occurrence of NLO responses in ferroelectric LC (FLC) has been demonstrated for several calamitic FLC built from rod-like mesogens³ but also more recently from bent-core mesogens⁴ with the experimental determination of NLO coefficients in the 10–100 pm V⁻¹ range.^{4b} FLC phases appear very attractive for potential applications in fast switching electro-optical devices and as switchable NLO materials. Among these, one of the most efficient mesogens contains a *p*-nitroaniline moiety, characterizing the push–pull effect, implanted into the rigid core in such a way that large components of the first hyperpolarizability (β) tensor are perpendicular to the molecular axis.^{3b} Thus, the molecular structures of LC molecules are still quite simple, and there remains plenty of room for optimizing the structures in order to maximize the NLO properties in view of targeted applications. For instance, Soldera et al.⁵ proposed in 2003 to attach a chiral sulfinate center directly on the NLO-phore, and a subsequent theoretical investigation was carried out to assess

the impact of substituting the phenyl ring bearing the sulfinate group by donor and acceptor groups.⁶ Such a procedure was not applied to banana-shaped mesogens, though their study constitutes an actual new field of LC research. Additionally, the recent experimental determination of NLO coefficients up to 100 pm V⁻¹ for bent-core LC fosters the interest to investigate their NLO properties, looking for larger β tensor components as well as structure–property relationships.

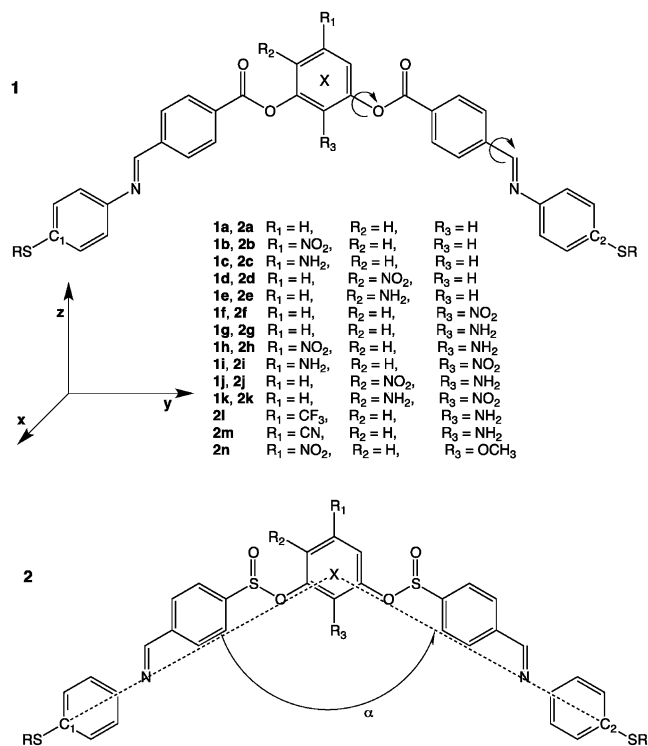
In this paper, the structure–NLO property relationships are derived for two series of banana-shaped mesogens bearing a pair of sulfinate or carboxyl groups between the NLO-phore and the rigid arms (Scheme 1). Second harmonic generation (SHG) responses in bent-core LC were addressed by several groups,^{4–7} in order to reveal the splayed polarization orientation. For instance, the study of Takezoe and co-workers^{7a} concerned a bent-core LC similar to compound **1a** where the terminal SR groups are replaced by SR* moieties with * standing for the presence of chirality. As a follow-up to our recent investigation in LC calamitics,⁶ the goal here is to address the variations in the β tensor components and related second-order NLO measurable quantities as a function of the position of the NH₂ donor and NO₂ acceptor groups, for bent-shaped molecules. These groups are actual prototype to address the effect of different push–pull moieties on the values of β .

Received: January 3, 2012

Revised: March 2, 2012

Published: March 5, 2012

Scheme 1. Sketch of the Molecular Structures 1 and 2 ($R = H$) as well as Definitions of the Molecular Cartesian Axes, of the C1–X–C2 Opening Angle (α), and of the Two Dihedral Angles Involved in Conformational Modifications



Additionally, considering the sulfonate and carboxyl groups aims to compare their effect on the NLO properties. Such a comparison was not feasible with calamitic chiral smectogens,⁶ since only the sulfonate group holds the chirality leading to the implicit noncentrosymmetry. Finally owing to their V-shape (or Λ -shape), there is an interest to address the variations of β as a function of a characteristic structural parameter, the α angle between the two conjugated arms.⁸

An inherent link between the mesogens structures and the macroscopic properties is actually far to be established. An actual small change in the molecular architecture of the mesogen can greatly affect the thermal stability of the mesophases.^{5,9} Alterations brought to the original molecules that display in their polymorphism the expected ferroelectric mesophase definitely yield a different LC polymorphism. Such a large chemical sensitivity to the occurrence of this particular mesophase cannot be clearly predicted. However, the bending angle, α , is a significant molecular characteristic that helps to distinguish between two kinds of compounds. A value of α approaching 60° gives rise to V-shaped molecules usually associated, like rod-like mesogens, with the calamitic mesophases or even the B4 phase.¹⁰ If α is about 120° , banana-shaped molecules (literally, these also correspond to V-shaped molecules with larger opening angle) are obtained yielding a great variety of molecular arrangements mainly depending on the polar direction, on the tilt direction, and on the phase chirality. Determination of this bending angle, α , must thus be considered in our calculations, and its link with the NLO coefficients can guide the effort in the design of new high performing molecules.

The paper is organized as follows. The section II describes the theoretical methods and the related computational aspects.

Then, in section III the results are presented and discussed before conclusions are drawn in section IV.

II. THEORETICAL AND COMPUTATIONAL ASPECTS

The molecular structures were optimized in vacuo at the density functional theory (DFT) level of approximation using the B3LYP hybrid exchange-correlation functional and the 6-31G* basis set. The first hyperpolarizabilities were determined at the HF response theory level, more precisely by adopting the time-dependent Hartree–Fock (TDHF)¹¹ and the coupled-perturbed Hartree–Fock (CPHF) schemes for obtaining the dynamic (or frequency-dependent) and static values, respectively. For the former, we considered an incident wavelength of 1064 nm ($\hbar\omega = 1.165$ eV). For a selection of compounds, in order to account for correlation effects on the static first hyperpolarizabilities, the second-order Møller–Plesset (MP2) method was employed in combination with the finite field (FF) procedure¹² implying a Romberg scheme to improve the accuracy on the numerical derivatives.¹³ FF/MP2 calculations were already shown to provide reliable first hyperpolarizabilities for organic chromophores because, in many cases, MP2 recovers the largest part of the electron correlation effects, as estimated from higher-order methods.¹⁴ In addition static and frequency-dependent hyperpolarizability calculations were also performed using a long-range corrected XC functionals, LC-BLYP with the $\mu = 0.47$ parameter. Although its advantages with respect to the TDHF method are not completely clarified,¹⁵ long-range corrected functionals have been shown to correct conventional DFT schemes for their shortsightedness drawbacks.¹⁶ The β calculations employed the 6-31+G* basis set, which was shown to be a good compromise between accuracy and computational resources for π -conjugated molecules bearing donor and acceptor groups.

Though for SHG, the $\beta(-2\omega; \omega, \omega)$ tensor contains 18 independent elements, representative tensor elements and averages have been considered, (i) the $\beta_{zzz}(-2\omega; \omega, \omega)$ tensor component, (ii) the $\beta_{HRS}(-2\omega; \omega, \omega)$ hyper-Rayleigh scattering (HRS) response, and (iii) the $\beta_{||}(-2\omega; \omega, \omega)$ quantity, which can be deduced from electric field-induced second harmonic generation (EFISHG) measurements. $\beta_{HRS}(-2\omega; \omega, \omega)$ is in fact related to the intensity of the vertically polarized (along the Z axis) scattered signal at 90° with respect to the propagation direction for a nonpolarized incident signal and is given by

$$\beta_{HRS}(-2\omega; \omega, \omega) = \sqrt{\langle \beta_{ZZZ}^2 \rangle + \langle \beta_{ZXX}^2 \rangle} \quad (1)$$

The depolarization ratio, DR, is then introduced, in order to reveal the shape of the NLO-phore

$$DR = \frac{I_{VV}^{2\omega}}{I_{HV}^{2\omega}} = \frac{\langle \beta_{ZZZ}^2 \rangle}{\langle \beta_{ZXX}^2 \rangle} \quad (2)$$

where $\langle \beta_{ZZZ}^2 \rangle$ and $\langle \beta_{ZXX}^2 \rangle$ are orientational averages of the β tensor, which are proportional to the scattered signal intensities for vertically and horizontally polarized incident signals, respectively. The quantities in eqs 1 and 2 were calculated without assuming Kleinman's conditions (full expressions of these terms can be found in ref 17). On the other hand,

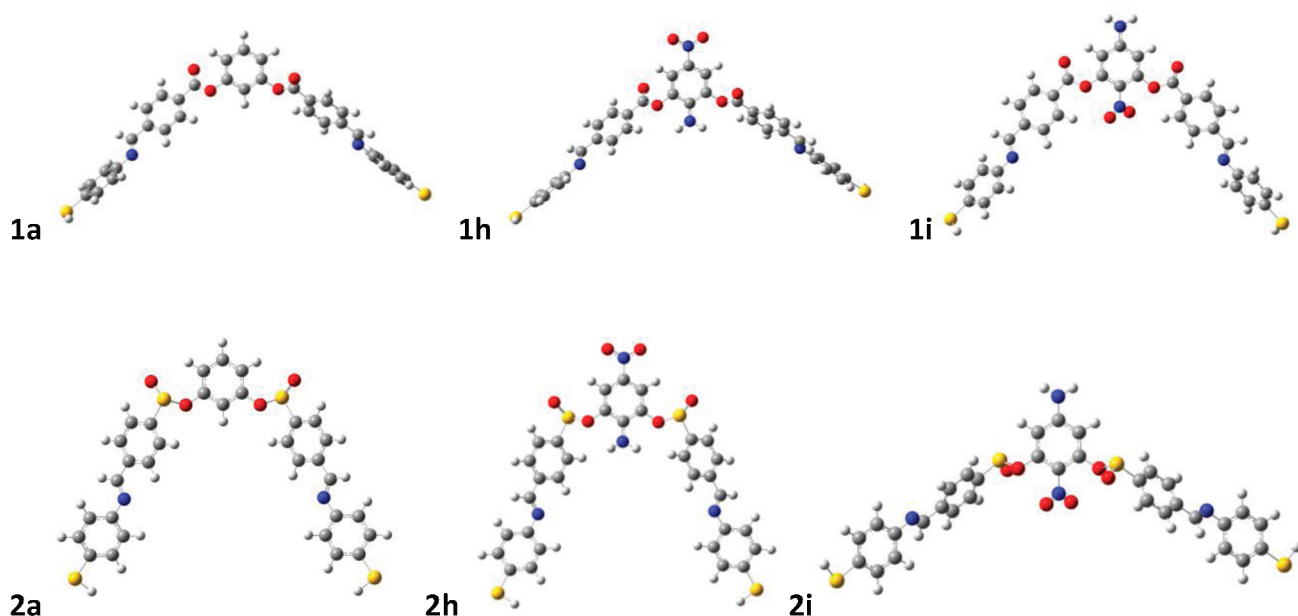


Figure 1. B3LYP/6-31G* optimized structures of 1a, 1h, 1i, 2a, 2h, and 2i, evidencing the range of opening angles.

$\beta_{\parallel}(-2\omega; \omega, \omega)$ corresponds to the projection of the vector part of β on the dipole moment vector

$$\begin{aligned}\beta_{\parallel}(-2\omega; \omega, \omega) &= \beta_{\parallel} \\ &= \frac{1}{5} \sum_i \frac{\mu_i}{\|\mu\|} \sum_j (\beta_{ijj} + \beta_{jij} + \beta_{jji}) \\ &= \frac{3}{5} \sum_i \frac{\mu_i \beta_i}{\|\mu\|}\end{aligned}\quad (3)$$

where $\|\mu\|$ is the norm of the dipole moment and μ_i and β_i are the components of the μ and β vectors, respectively. All calculations were performed using *Gaussian 09*¹⁸ as well as homemade codes to carry out the FF Romberg differentiation procedure.

III. RESULTS AND DISCUSSION

III.A. Sulfinate versus Carboxyl Moieties. B3LYP/6-31G* geometry optimizations demonstrate that changing the substituents on the central phenyl ring has an impact on the shape of the molecule and particularly on its opening angle α (Figure 1, Table 1). The actual effect of substituting the carboxyl group by the sulfinic group greatly influences this bending angle. Although for carboxyl derivatives, α ranges from 94° to 117°, for sulfinic molecules, it goes from 69° to 139° (Table 1). This difference is particularly noticeable for the bare molecule (1a) for which α is lessened to a great extent giving for 2a a value of 75.9°, which approaches the 60° angle used to define V-shaped molecules.^{10a} The presence of a group at the R₁ position (2b and 2c), i.e., at the apex of the V-shaped molecule, naturally confirms such a tendency (Scheme 1). Conversely, for the sulfinate series, the location of a group at the R₃ position (2f and 2g), i.e., at the para position of the R₁ group, increases the aperture, leading to α slightly superior to the value expected for banana-shaped molecules. The effect of different NLO-phore substitutions on the value of α (Table 1) can be regarded more explicitly. For the carboxyl series, fluctuations of α in the 107 ± 10° range cannot yield significant

conclusions. Moreover, it can be noticed that for both series that any substitution at the R₁ position only (1b, 2b, 1c, and 2c) does not seriously affect the bending angle, comparatively to the bare molecule (1a, 2a). On the other hand, for the

Table 1. SHG First Hyperpolarizability of 1a–1k and 2a–2n Compounds As Calculated at the TDHF/6-31+G* Level of Approximation for a Wavelength of 1064 nm^a

	β_{zzz}	β_{\parallel}	β_{HRS} (DR)	α
1a	−2531	3748	2783 (4.10)	106.6
1b (R ₁ = NO ₂)	−3116	4474	3310 (4.15)	108.5
1c (R ₁ = NH ₂)	−2645	−1261	2665 (4.29)	101.8
1d (R ₂ = NO ₂)	−2408	3152	3497 (3.53)	111.0
1e (R ₂ = NH ₂)	−2926	188	2659 (4.56)	101.8
1f (R ₃ = NO ₂)	−4286	−4903	3357 (5.25)	96.6
1g (R ₃ = NH ₂)	−2390	3146	2753 (4.00)	109.4
1h (R ₁ = NO ₂ , R ₃ = NH ₂)	−3840	4733	3376 (4.64)	111.4
1i (R ₁ = NH ₂ , R ₃ = NO ₂)	−3849	−4480	3107 (5.16)	93.6
1j (R ₂ = NO ₂ , R ₃ = NH ₂)	−1914	3218	3362 (3.39)	115.6
1k (R ₂ = NH ₂ , R ₃ = NO ₂)	−1484	−2402	2747 (3.04)	117.0
2a	−4961	3636	2358 (6.51)	75.9
2b (R ₁ = NO ₂)	−6498	4620	3016 (6.35)	75.5
2c (R ₁ = NH ₂)	−4332	2985	2121 (6.45)	77.2
2d (R ₂ = NO ₂)	−3255	3135	2806 (4.27)	104.2
2e (R ₂ = NH ₂)	−1463	1173	1660 (2.49)	132.5
2f (R ₃ = NO ₂)	−581	−2326	2098 (2.81)	124.8
2g (R ₃ = NH ₂)	−1398	739	1278 (2.45)	138.7
2h (R ₁ = NO ₂ , R ₃ = NH ₂)	−8302	5239	3536 (5.57)	68.9
2i (R ₁ = NH ₂ , R ₃ = NO ₂)	50	−1993	2046 (2.42)	124.5
2j (R ₂ = NO ₂ , R ₃ = NH ₂)	−3701	3366	2792 (4.64)	101.3
2k (R ₂ = NH ₂ , R ₃ = NO ₂)	−1798	−2280	2082 (2.80)	102.4
2l (R ₁ = CF ₃ , R ₃ = NH ₂)	−6317	4179	2785 (5.89)	69.2
2m (R ₁ = CN, R ₃ = NH ₂)	−7251	4740	3163 (5.83)	69.8
2n (R ₁ = NO ₂ , R ₃ = OCH ₃)	−5884	4247	2879 (6.28)	71.8

^aAll values are given in atomic units (1 a.u. of β = 3.6213 × 10^{−42} m⁴ V^{−1} = 3.206361 × 10^{−53} C³ m³ J^{−2} = 8.6392 × 10^{−33} esu) within the T convention.²⁰ The opening angles (in degrees) are given in the last column.

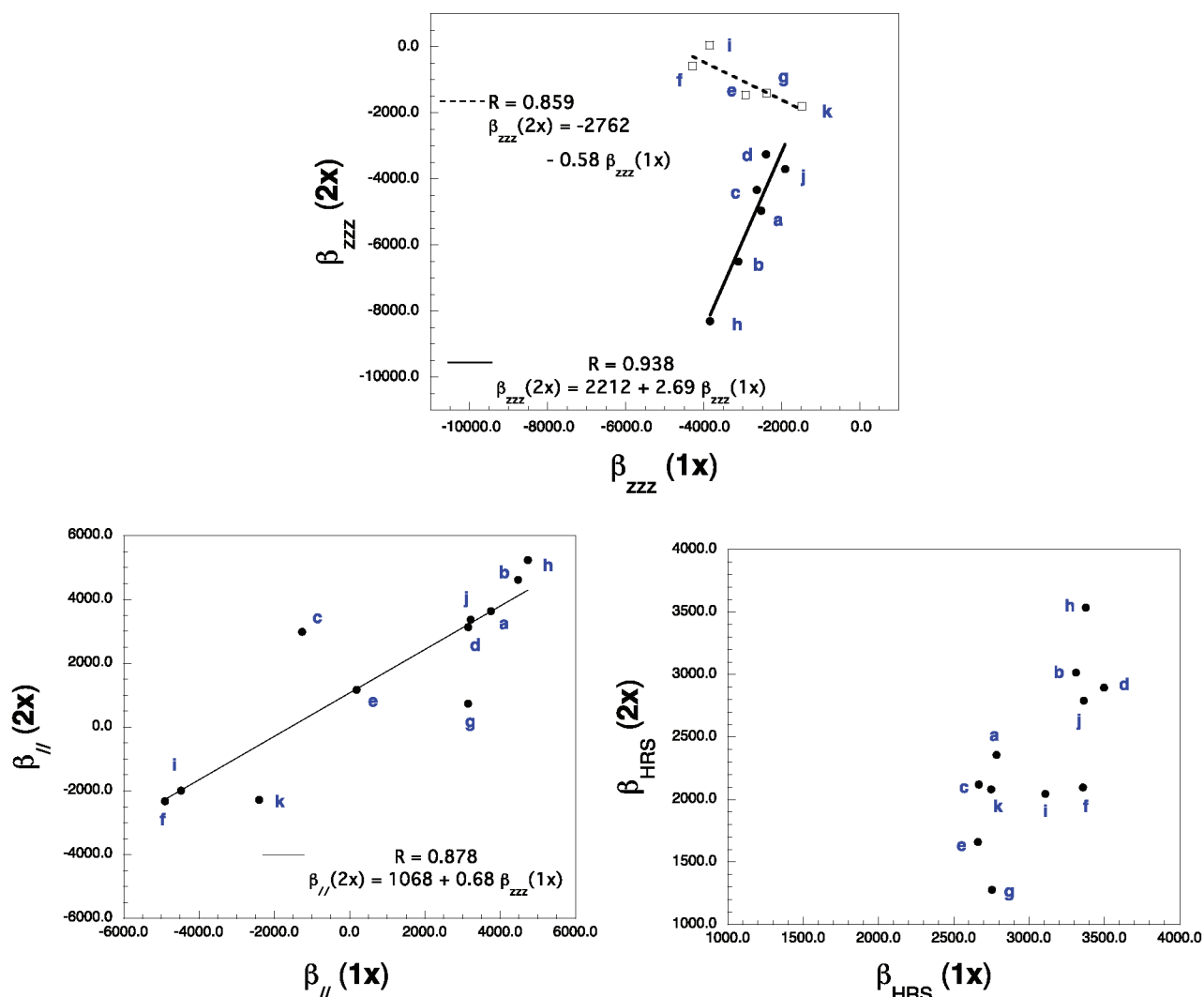


Figure 2. Relationships between the β_{zzz} , $\beta_{||}$, and β_{HRS} values for the **1x** (carboxyl) and **2x** (sulfonate) compound families as determined from TDHF/6-31+G* calculations.

sulfonate molecules, the presence of a group at the R_3 location increases the interactions between the wings leading to a large value of α (**2f** and **2g**). Such an effect is stronger when R_3 is the amino group for which $\alpha = 139^\circ$ (**2g**), whereas it remains significant when the nitro group is positioned at the para position and $\alpha = 125^\circ$ (**2i**). Nevertheless, reversing the order of these groups at the R_1 and R_3 positions (**2h**) yields the lowest bending angle of the series, $\alpha = 69^\circ$, which closely approaches the value usually found in V-shaped calamitic molecules. The direction of the push–pull assembly can thus also greatly influence the aperture of the wings in V-shaped molecules, and consequently the very existence of the banana-shaped mesophase. Such conclusions can also be established from the study of the α dependence on substitutions at the R_2 position, i.e. at the ortho position of R_1 . For the carboxyl series α does not explicitly depend on the position of the nitro and amino groups at the R_1 and R_2 positions. This is no more the case for the sulfonate series, for which the amino group at R_2 (**2e**) gives a large value for α . Finally, when R_1 and R_3 are amino or nitro groups, the value of α does not depend on their relative position. This important contrast between the two series is also disclosed in the NLO calculations.

Figure 2 displays the relationships between the first hyperpolarizabilities of the carboxyl (**1x**) and sulfonate (**2x**) families as determined at the TDHF/6-31+G* level of approximation. As for the aperture angle, much different conclusions between the two series can be drawn for the different β quantities. β_{zzz} of the **2x** compounds are strongly modified by the nature and the position of the donor/acceptor substituents and vary from about 0 to -8000 au whereas the β_{zzz} variations of **1x** occur in a narrower range, between -1400 and -4300 au. In fact, the compounds can be classified into two categories. In the first category (**e**, **f**, **g**, **i**, and **k**), R_2 is a donor group or R_3 is an acceptor group so that the amplitude of β_{zzz} is rather small for the **2x** compounds. In that case when the β_{zzz} amplitude increases for the **1x** family, it decreases for the **2x** compounds, confirming the antagonistic role of the SO_2 and CO_2 moieties. In the second group (**a**, **b**, **c**, **d**, **h**, and **j**), where the charge transfer goes in the direction from R_3 to R_1 , the amplitude of β_{zzz} increases simultaneously for both the **1x** and **2x** families, though faster in the **2x** family. Turning to the $\beta_{||}$ quantities, the orientation of the dipole moment is playing now a role and a linear relationship appears between the two sets of values. Nevertheless, contrary to β_{zzz} , the range of $\beta_{||}$ value is

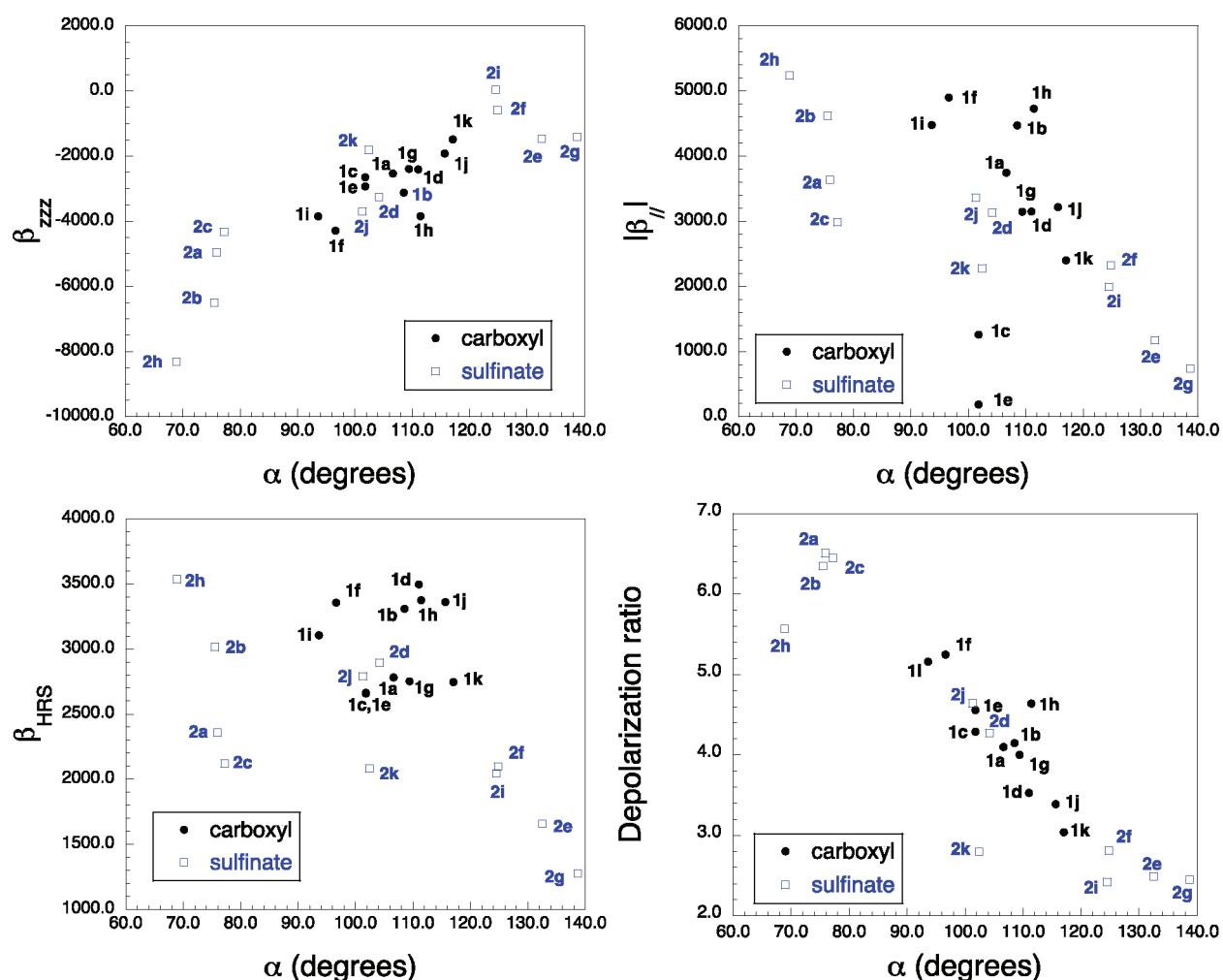


Figure 3. Behavior of the β_{zzz} , $\beta_{||}$, β_{HRS} , and DR values for the $1x$ (carboxyl) and $2x$ (sulfinate) compound families as determined from TDHF/6-31+G* calculations, with respect to the bending angle α value.

broader for the $1x$ family. This demonstrates that the donor/acceptor effects of the carboxyl group are stronger than those of the sulfinate moiety. Finally, the reverse trend between the two families is observed in the case of the HRS quantities, showing now the importance of the β tensor components that do not contribute to $\beta_{||}$, i.e., to the vector component of β along the dipole moment. This argument is supported by the broader range of the depolarization ratios in the $2x$ family, whereas DR of the $1x$ family is generally within the 4–5 range, corresponding to one-dimensional NLO-phores.¹⁹

To uncover any correlation between α and the NLO properties, calculated first hyperpolarizabilities are reported with respect to the aperture angle (Figure 3). Absolute values are considered for $\beta_{||}$ in order to reveal only the behavior of the modulus. Dependency of β_{zzz} and DR with α is clearly observed for both series, whereas for $|\beta_{||}|$ values a linear relationship is monitored for the sulfinate compounds only. No actual trend is displayed for β_{HRS} values. The DR values of the carboxyl family are generally smaller than 5, with the smallest DR values corresponding to the largest α angles and vice versa. The situation is different for the sulfinate family where the aperture angles are either smaller than 80° or larger than 100°. In the former case, DR is larger than 5, if not 6, while in the latter case, DR gets smaller and even of the order of 2.4–3.0 when $\alpha > 120^\circ$. These variations are consistent with the analysis made in

ref 8d on V-shaped NLO compounds, where the β_{zxz}/β_{zzz} is shown to increase with α as well as with the donor/acceptor strength. A linear relationship between α and β_{zzz} is also observed. However, for the sulfinate series a distinction is made according to the group attached to the molecule: as previously mentioned, a donor group (amine) increases the bending angle, and thus reduces the value of β_{zzz} . This distinction is not observed for the carboxyl series for which α presents smaller variations. There is also a clear correlation between the variations of α going from the carboxyl to the sulfinate families and those of β_{zzz} of the two categories of molecules highlighted in Figure 2a. Indeed, α decreases in the first category (a, b, c, d, h, and j) but increases for the other one (i, f, e, and g), leading to increases or decreases of the β_{zzz} amplitude, respectively. Only **1k/2k** ($R_2 = \text{NH}_2$ and $R_3 = \text{NO}_2$) is an exception but its value is at the intersection of both lines on Figure 2. This highlights the double impact of the substituents on the first hyperpolarizabilities, a direct impact associated with the variations of the electronic properties and an indirect effect relayed by the modification of the geometry and the aperture angle in particular.

III.B. Donor/Acceptor Effects. If just considering the amino/nitro substituent pair on the central phenyl ring, it is obvious that the largest β responses are obtained when the substituents are placed in para position. Indeed, in that case,

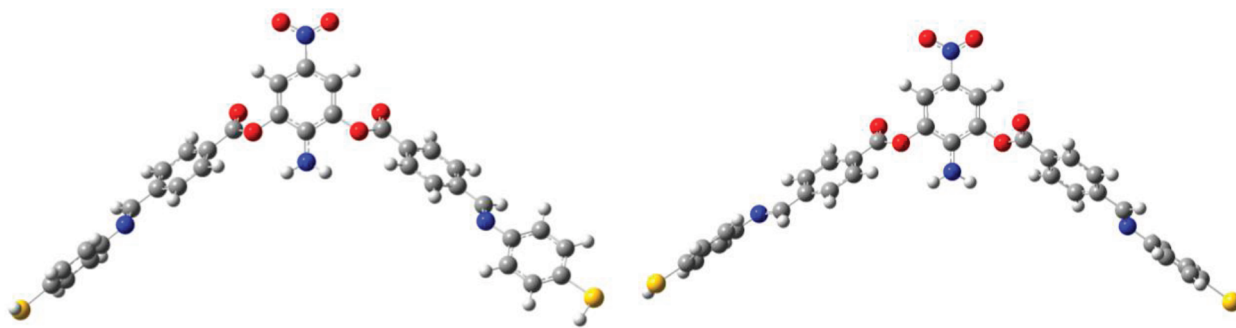


Figure 4. Alternative conformations of **1h** as obtained from B3LYP/6-31G* geometry optimizations. The left structure is obtained by rotating around the C–O bond while the right one by rotation around the C(Ph)–C(=N) bond.

Table 2. SHG First Hyperpolarizability of Three Conformers of **1h** As Calculated at the TDHF/6-31+G* Level of Approximation for a Wavelength of 1064 nm^a

	β_{zzz}	$\beta_{ }$	β_{HRS} (DR)	α
1h	−3840	4733	3376 (4.64)	111.4
1h with the two C=O parallel	−4002	4892	3412 (5.10)	108.8
1h with rotation around C(Ph)—C(=N)	−2948	4184	3212 (4.15)	116.8

^aAll values are given in atomic units.

β_{HRS} , as estimated from TDHF/6-31+G* calculations, is more than 5 times larger than for its ortho and meta isomers. For $\beta_{||}$, the difference is even bigger. This *p*-nitroaniline core is present in the **1h** and **1i** as well as **2h** and **2i** compounds, which enables to probe the role of the carboxyl- and sulfinate-based lateral groups. When placed in ortho position of the NH₂ group, the sulfinate group leads to a substantial enhancement of the β quantities whereas in the opposite case, when placed in ortho of the nitro group, the β_{zzz} component almost vanishes, leading to large reductions of $\beta_{||}$ and β_{HRS} . Though the presence of the amino group in R₃ reduces α , and therefore enhances the β_{zzz}/β_{xxx} ratio, these data enable to attribute a donor character to the sulfinate-based arms. A similar conclusion is drawn when using the bare mesogen (**2a**) as reference structure, of which the large and negative β_{zzz} tensor component demonstrates the direction of charge-transfer and hyperpolarization. Indeed, when adding an acceptor group in R₁ (**2b**) β increases, whereas the opposite is observed when R₁ = NH₂ (**2c**). The other compounds of the sulfinate family display intermediate behavior and β amplitudes, including the **2j** and **2k** molecules, where the donor and acceptor characters of the amino and nitro groups are less effective since they are in meta position.

These donor/acceptor effects have to be regarded concurrently with the value of the aperture angle. An important value of β_{zzz} for **2h** corresponds to a very low aperture of the wings (68.9°), which makes the material less likely to exhibit a banana phase by varying the temperature. Conversely, **2i**, which exhibits a very low value of β_{zzz} , has better chance to exhibit such a mesophase in its polymorphism.

Turning now to the carboxyl-based mesogens, the smaller β_{zzz} value of the bare compound (**1a**) with respect to **2a** shows that the donor role of the carboxyl group is weaker than the donor character of the sulfinate group in **2a**. Moreover, switching the NH₂/NO₂ groups in R₁/R₃ positions has a reduced impact on the β quantities, but influences α , showing that the direct and indirect effects compensate each other. Thus **1h**, with an aperture angle of 111.4°, is more likely to exhibit a banana phase, than **1i**, for which α is equal to 93.6°. The same effect is encountered for **1f**, which only contains a nitro group

in R₃. It actually displays the largest β_{zzz} response in that family but possesses an aperture angle of 96.6°.

Additional donor/acceptor effects were investigated by considering the **2h** structure and by replacing the nitro group in R₁ by a trifluoromethyl (**2l**) or by a cyano (**2m**) group or by substituting the amino group in R₃ by a methoxy group (**2n**) but they do not lead to enhanced hyperpolarizabilities with respect to **2h** (Table 1). Moreover, their aperture angle of the order of 70° does not match with the expected geometric characteristic of molecules that exhibit banana phase.

III.C. Conformational Effects. The studied mesogens can exist under different conformations. Therefore, we have taken compound **1h** as reference and have considered two types of rotation around dihedral angles, in order to probe first their relative energies and then their first hyperpolarizabilities (Figure 4). The first conformer is obtained by rotating around one of the C–O bonds in such a way that the two C=O bonds point in the same direction. Doing so, after B3LYP/6-31G* geometry optimization the energy is only 0.8 kJ/mol higher. As presented in Table 2, this leads to a small increase of the first hyperpolarizability (less than 5%). The other change of conformation is carried out by rotating around the C(Ph)—C(=N) bond, achieving a very similar energy (+ 0.4 kJ/mol). Again, the change in β_{HRS} is negligible (−5%) but the variations in β_{zzz} and $\beta_{||}$ are larger since this structural change modifies α and the β_{zzz}/β_{xxx} ratio. Though for describing the first hyperpolarizability of these mesogens it would be needed to average over the different conformers using Boltzmann distribution weights in the canonical ensemble, the small variations of the hyperpolarizabilities, except β_{zzz} to some extent, enable to assess the performance of the different species by considering the most stable conformer.

III.D. Impact of the Method of Calculation. The impact of the method of calculation on the hyperpolarizability values has been probed by comparing the frequency-dependent β values obtained using the TDHF/6-31+G* values (Table 1) with those evaluated at the TDDFT/LC-BLYP/6-31+G* level (Table 3) as well as by comparing the static CPHF/6-31G* results with the static ones obtained within LC-BLYP/6-31G*

Table 3. SHG First Hyperpolarizability of 1a–1k and 2a–2k Compounds As Calculated at the TDDFT/LC-BLYP/6-31+G* Level of Approximation for a Wavelength of 1064 nm^a

	β_{zzz}	$\beta_{ }$	β_{HRS} (DR)
1a	−2918	4376	3248 (4.11)
1b	−3769	5470	4032 (4.19)
1c	−3323	106	3028 (4.58)
1d	−3032	4092	4249 (3.65)
1e	−2995	−1702	3080 (4.28)
1f	−4992	−5815	4000 (5.17)
1g	−2748	3704	3189 (4.01)
1h	−4920	5936	4183 (4.83)
1i	−4216	−5140	3615 (4.94)
1j	−2425	4101	4043 (3.50)
1k	−1681	−2575	3188 (3.06)
2a	−5608	4276	2765 (6.60)
2b	−7599	5643	3657 (6.56)
2c	−4822	3519	2453 (6.51)
2d	−3913	3988	3336 (4.23)
2e	−1568	1437	1896 (2.56)
2f	−808	−2859	2523 (2.91)
2g	−1602	1012	1549 (2.49)
2h	−10068	6579	4381 (5.88)
2i	60	−2343	2395 (2.43)
2j	−4400	4203	3349 (4.60)
2k	−2197	−2692	2405 (2.91)

^aAll values are given in atomic units within the T convention.

and MP2/6-31G* methods (Table 4). As illustrated in Figure 5, the TDDFT/LC-BLYP and TDHF methods predict similar variations of β_{HRS} and $\beta_{||}$ as a function of the number, the nature, and the position of the donor/acceptor substituents, described by linear regressions with correlation coefficients close to 1. Although not shown here, a similar agreement is found for the β_{zzz} quantities.

Moreover, as listed in Table 4, the HF and LC-BLYP values are much similar and differ, with a few exceptions, from the MP2 results by 15–50%. For β_{zzz} (besides β_{zzz} of 2i, which is small with all methods), $\beta_{||}$, and β_{HRS} , the values satisfy the HF < LC-BLYP < MP2 ordering. We also note that the MP2/HF ratios are slightly larger in the case of the best push–pull π -conjugated systems, 1h and 2h, in comparison to the bare compounds (1a and 2a) and, to a lower extent, 1i and 2i where the NO₂/NH₂ charge transfer axis is opposite. More importantly, these electron correlation effects are similar for the different compounds, with a MP2/HF ratios that varies by 10% or less, demonstrating that the HF (and also LC-BLYP) values are sufficient to assess structure–property relationships. These electron correlation effects, including the performance of LC-BLYP with respect to the HF and MP2 methods, are in agreement with recent studies.^{15,16} In addition, the B3LYP approach predicts β responses 2 to 3 times larger than those calculated at the MP2 level, evidencing the effects of shortsightedness of this exchange–correlation functional that only contains 20% of HF exchange. There is also a very good agreement on the DR values obtained at the HF, LC-BLYP, and MP2 levels of approximation, showing that the dimensionality of the NLO-phore is consistently predicted by the three methods. These comparisons justify the use of the TDHF method to deduce structure–property relationships in sections IIIA through III-C.

Table 4. Static First Hyperpolarizability of Selected Compounds As Calculated at the HF/6-31G*, LC-BLYP/6-31G*, and MP2/6-31G* Levels of Approximation^a

	β_{zzz}	$\beta_{ }$	β_{HRS} [DR]
Hartree–Fock			
1a	−1672 (1.22)	2227 (1.29)	1625 (1.30) [4.23]
1h	−2551 (1.39)	2835 (1.45)	1972 (1.45) [4.95]
1i	−2250 (1.20)	−2639 (1.26)	1852 (1.28) [4.87]
2a	−2869 (1.20)	2162 (1.32)	1391 (1.32) [6.60]
2h	−4878 (1.36)	3117 (1.47)	2091 (1.43) [5.57]
2i	131 (−0.08)	−1183 (1.41)	1232 (1.34) [2.38]
LC-BLYP			
1a	−1727 (1.18)	2353 (1.22)	1718 (1.23) [4.22]
1h	−2802 (1.27)	3126 (1.31)	2165 (1.32) [5.03]
1i	−2215 (1.22)	−2712 (1.22)	1929 (1.23) [4.67]
2a	−2918 (1.19)	2293 (1.24)	1472 (1.24) [6.66]
2h	−5206 (1.27)	3438 (1.33)	2279 (1.32) [5.86]
2i	140 (−0.06)	−1251 (1.33)	1297 (1.28) [2.38]
B3LYP			
1a	−5864 (0.35)	8341 (0.34)	6109 (0.34) [4.18]
1h	−7310 (0.49)	10005 (0.41)	7285 (0.39) [4.30]
1i	−9369 (0.29)	−10362 (0.32)	7157 (0.33) [5.23]
2a	−11204 (0.31)	8936 (0.32)	5732 (0.32) [6.70]
2h	−17004 (0.39)	11820 (0.39)	7715 (0.39) [6.23]
2i	−1038 (0.01)	−5450 (0.31)	5027 (0.33) [2.74]
MP2			
1a	−2035	2864	2105 [4.15]
1h	−3547	4097	2852 [4.95]
1i	−2693	−3312	2372 [4.63]
2a	−3465	2848	1831 [6.63]
2h	−6621	4583	2997 [6.22]
2i	−8	−1665	1657 [2.49]

^aValues in parentheses correspond to the MP2/Method-X ratios. All values are given in atomic units within the T convention.

IV. CONCLUSION

The first hyperpolarizability of two series of molecules with bent-shaped structures has been calculated at ab initio levels. These two series consist in carboxyl derivatives for which some molecules are known to exhibit banana phases (for instance, B3 and B7 phases for the bare molecule with eight carbon atoms in the alkyl chains²¹), and in their sulfinate homologues that have not been synthesized yet. The final purpose is to reveal the relevance or not in synthesizing these latter molecules. The strategy is based on reporting the effect of the positions of donor and acceptor groups on the central benzene ring on the structural parameters and on the first hyperpolarizabilities. The angle between the two structural arms serves to identify the occurrence of liquid crystalline phases. Calculations reveal that it strongly depends on the presence of substituents in the sulfinate series. As a consequence, in addition to the direct effect of the substituents on the first hyperpolarizabilities, the change of geometry in the sulfinate family must be considered as a critical indirect effect. In the carboxyl family, appropriate substitution by a pair of push–pull substituents leads to an enhancement of the first hyperpolarizability by about 20% while keeping an opening angle close to 110°. On the other hand, similar substitutions on the sulfinate derivatives can result in a larger increase of the first hyperpolarizability, owing to the donor character of the sulfinate group, but it is detrimental to the geometry since the aperture of the molecular arms is close to 70°.

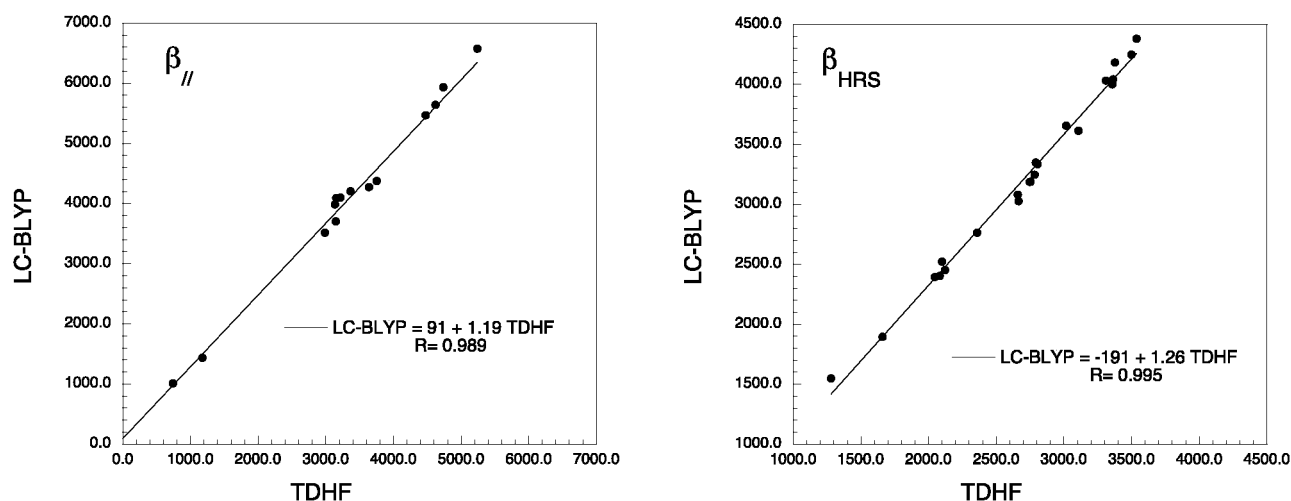


Figure 5. Relationship between the TDDFT/LC-BLYP/6-31+G* and TDHF/6-31+G* methods for the β_{\parallel} (left) and β_{HRS} (right) quantities.

As a conclusion, we have shown that the combination of characteristic geometrical data stemming from experiment with calculations is a powerful tool to guide the development toward banana-shaped molecules for applications in liquid crystals with large NLO properties. In particular, we show here that sulfinate molecules are not expected to be good candidates for such applications.

AUTHOR INFORMATION

Corresponding Author

*Email: benoit.champagne@fundp.ac.be (B.C.). Email: armand.soldera@usherbrooke.ca (A. S.).

Notes

The authors declare no competing financial interest.

ACKNOWLEDGMENTS

The authors are grateful to the CFI, NSERC, C  MOPUS (Universit   de Sherbrooke), the Minist  re des Relations Internationales du Qu  bec, and the Direction g  n  rale des Relations Ext  rieures de la R  gion wallonne de Belgique, through the cooperation Qu  bec/Wallonie ST-8/04.808 program. The calculations were performed on the Interuniversity Scientific Computing Facility (ISCF) installed at the Facult  s Universitaires Notre-Dame de la Paix (Namur, Belgium), for which we gratefully acknowledge financial support of the FNRS-FRFC (Convention No. 2.4.617.07.F), and of the FUNDP.

REFERENCES

- (1) (a) Walba, D. M. *Materials-Chirality: Vol. 24 of Topics in Stereochemistry*; Green, M. M., Nolte, R. J. M., Meijer, E. W., Eds.; John Wiley & Sons: New York, 2003; pp 457–518. (b) Amanaratha Reddy, A.; Tschierke, C. *J. Mater. Chem.* **2006**, *16*, 907–961. (c) Takezoe, H.; Takanishi, Y. *Jpn. J. Appl. Phys.* **2006**, *45*, 597–625. (d) Kohout, M.; Svoboda, J.; Novotna, V.; Pociecha, D. *Liq. Cryst.* **2011**, *38*, 1099–1110.
- (2) Niori, T.; Sekine, T.; Watanabe, J.; Furukawa, T.; Takezoe, H. *J. Mater. Chem.* **1996**, *6*, 1231–1233.
- (3) (a) Walba, D. M.; Ros, M. B.; Clark, N. A.; Shao, R.; Robinson, M. G.; Liu, J. Y.; Johnson, K. M.; Doroski, D. *J. Am. Chem. Soc.* **1991**, *113*, 5471–5474. (b) Schadt, M.; Schmitt, K. *Appl. Phys. B: Laser Opt.* **1994**, *59*, 607–615. (c) Walba, D. M.; Dyer, D. J.; Sierra, T.; Cobben, P. L.; Shao, R.; Clark, N. A. *J. Am. Chem. Soc.* **1996**, *118*, 1211–1212. (d) Walba, D. M.; Xiao, L.; Keller, P.; Shao, R.; Link, D.; Clark, N. A. *Pure Appl. Chem.* **1999**, *71*, 2117–2123. (e) Zhang, Y.; Martinez-Perdiguero, J.; Baumeister, U.; Walker, C.; Etzebarria, J.; Prehm, M.; Ortega, J.; Tschierske, C.; O’Callaghan, M. J.; Harant, A.; Handschy, M. *J. Am. Chem. Soc.* **2009**, *131*, 18386–18392.
- (4) (a) Pintre, I. C.; Gimeno, N.; Serrano, J. L.; Ros, M. B.; Alonso, I.; Folcia, C. L.; Ortega, J.; Etzebarria, J. *J. Mater. Chem.* **2007**, *17*, 2219–2227. (b) Pintre, I. C.; Serrano, J. L.; Ros, M. B.; Martinez-Perdiguero, J.; Alonso, I.; Ortega, J.; Folcia, C. L.; Etzebarria, J.; Alicante, R.; Villacampa, B. *J. Mater. Chem.* **2010**, *20*, 2965–2971.
- (5) Soldera, A.; Th  berge, R. *Liq. Cryst.* **2003**, *30*, 1251–1254.
- (6) Perreault, F.; Champagne, B.; Soldera, A. *Chem. Phys. Lett.* **2007**, *440*, 116–120.
- (7) (a) Araoka, F.; Hoshi, H.; Takezoe, H. *Phys. Rev. E* **2004**, *69*, 051704. (b) Choi, E. J.; Cui, X.; Ohk, C. W.; Zin, C. W.; Lee, J. H.; Lim, T. K.; Jang, W. G. *J. Mater. Chem.* **2010**, *20*, 3743–3749.
- (8) (a) Moylan, C. R.; Ermer, S.; Lovejoy, S. M.; McComb, I.-H.; Leung, D. S.; Wortmann, R.; Krdmer, P.; Twieg, R. J. *J. Am. Chem. Soc.* **1996**, *118*, 12950–12955. (b) Yakimanski, A. V.; Kolb, U.; Matveeva, G. N.; Voigt-Martin, I.; Tenkovtsev, A. V. *Acta Crystallogr.* **1997**, *A53*, 603. (c) Ostroverkhov, V.; Petschek, R. G.; Singer, K. D.; Twieg, R. J. *Chem. Phys. Lett.* **2001**, *340*, 109–115. (d) Yang, M.; Champagne, B. *J. Phys. Chem. A* **2003**, *107*, 3942–3951. (e) Guthm  ller, J.; Simon, D. *J. Chem. Phys.* **2006**, *124*, 174502. (f) Zrig, S.; Koeckelberghs, G.; Verbiest, T.; Andrioletti, B.; Rose, E.; Persoons, A.; Asselberghs, I.; Clays, K. *J. Org. Chem.* **2007**, *72*, 5855–5858. (g) Koeckelberghs, G.; de Groof, L.; Perez-Moreno, J.; Asselberghs, I.; Clays, K.; Verbiest, T.; Samyn, C. *Tetrahedron* **2008**, *64*, 3772–3781. (h) Si, Y. L.; Liu, C. G.; Wang, E. B.; Su, Z. M. *Theor. Chem. Acc.* **2009**, *122*, 217–226. (i) Andreu, R.; Galan, E.; Garin, J.; Herrero, V.; Lacarra, E.; Orduna, J.; Alicante, R.; Villacampa, B. *J. Org. Chem.* **2010**, *75*, 1684–1692. (j) Sergeev, S.; Didier, D.; Boitsov, V.; Teshome, A.; Asselberghs, I.; Clays, K.; Vande Velde, C. M. L.; Plaquet, A.; Champagne, B. *Chem.—Eur. J.* **2010**, *16*, 8181–8190. (k) Coe, B. J.; Fielden, J.; Foxon, S. P.; Harris, J. A.; Helliwell, M.; Brunschwig, B. S.; Asselberghs, I.; Clays, K.; Garin, J.; Orduna, J. *J. Am. Chem. Soc.* **2010**, *132*, 10498–10512.
- (9) (a) Vadnais, R.; Beaudoin, M. A.; Soldera, A. *J. Chem. Phys.* **2008**, *129*, 164908. (b) Vadnais, R.; Beaudoin, M. A.; Beaudoin, A.; Heinrich, B.; Soldera, A. *Liq. Cryst.* **2008**, *35*, 357–364.
- (10) (a) Alonso, I.; Martinez-Perdiguero, J.; Ortega, J.; Folcia, C. L.; Etzebarria, J.; Gimeno, N.; Ros, M. B. *Liq. Cryst.* **2011**, *37*, 1465–1470. (b) Yelamagad, C. V.; Shashikala, I.; Shankar Rao, D. S.; Krishna Prasad, S. *Liq. Cryst.* **2004**, *31*, 1027–1032.
- (11) (a) Sekino, H.; Bartlett, R. J. *J. Chem. Phys.* **1986**, *85*, 976–989. (b) Karna, S. P.; Dupuis, M. *J. Comput. Chem.* **1991**, *12*, 487–504.
- (12) Cohen, H. D.; Roothaan, C. C. J. *J. Chem. Phys.* **1965**, *43*, S34.
- (13) (a) Davis, P. J.; Rabinowitz, P. *Numerical Integration*; Blaisdell Publishing Company: London, 1967; p 166. (b) See also for an example of the Romberg scheme in the case of push-pull π -conjugated

systems : Champagne, B.; Kirtman, B. in *Nonlinear Optical Materials, Vol. 9 of Handbook of Advanced Electronic and Photonic Materials and Devices*; Nalwa, H. S., Ed.; Academic Press: San Diego, CA, 2001; Chapter 2, pp 63–126.

(14) (a) Champagne, B.; Kirtman, B. *J. Chem. Phys.* **2006**, *125*, 024101. (b) Mançois, F.; Sanguinet, L.; Pozzo, J. L.; Guillaume, M.; Champagne, B.; Rodriguez, V.; Adamietz, F.; Ducasse, L.; Castet, F., J. *Phys. Chem. B* **2007**, *111*, 9795–9802. (c) de Wergifosse, M.; Champagne, B. *J. Chem. Phys.* **2011**, *134*, 074113.

(15) (a) Kamiya, M.; Sekino, H.; Tsuneda, T.; Hirao, K. *J. Chem. Phys.* **2005**, *122*, 234111. (b) Sekino, H.; Maeda, Y.; Kamiya, M.; Hirao, K. *J. Chem. Phys.* **2007**, *126*, 014107. (c) Jacquemin, D.; Perpète, E. A.; Medved, M.; Scalmani, G.; Frisch, M. J.; Kobayashi, R.; Adamo, C. *J. Chem. Phys.* **2007**, *126*, 191108. (d) Kirtman, B.; Bonness, S.; Ramirez-Solis, A.; Champagne, B.; Matsumoto, H.; Sekino, H. *J. Chem. Phys.* **2008**, *128*, 114108. (e) Limacher, P. A.; Mikkelsen, K. V.; Lüthi, H. P. *J. Chem. Phys.* **2009**, *130*, 194114. (f) Song, J. W.; Watson, M. A.; Sekino, H.; Hirao, K. *Int. J. Quantum Chem.* **2009**, *109*, 109, 1012.

(16) (a) Champagne, B.; Perpète, E. A.; Jacquemin, D.; van Gisbergen, S. J. A.; Baerends, E. J.; Soubra-Ghaoui, C.; Robins, K.; Kirtman, B. *J. Phys. Chem. A* **2000**, *104*, 4755–4763. (b) Plaquet, A.; Guillaume, M.; Champagne, B.; Rougier, L.; Mançois, F.; Rodriguez, V.; Pozzo, J. L.; Ducasse, L.; Castet, F. *J. Phys. Chem. C* **2008**, *112*, 5638–5645. (c) Suponitsky, K. Y.; Tafur, S.; Masunov, A. E. *J. Chem. Phys.* **2008**, *129*, 044109. (d) Lu, S. I.; Chiu, C. C.; Wang, Y. F. *J. Chem. Phys.* **2011**, *135*, 134104. (e) Plaquet, A.; Champagne, B.; Ducasse, L.; Bogdan, E.; Castet, F.; AIP Conf. Proceedings, in press.

(17) Bersohn, R.; Pao, Y. H.; Frisch, H. L. *J. Chem. Phys.* **1966**, *45*, 3184–3198.

(18) Frisch, M. J.; Trucks, G. W.; Schlegel, H. B.; Scuseria, G. E.; Robb, M. A.; Cheeseman, J. R.; Montgomery, J. A.; Vreven, T.; Kudin, K. N.; Burant, et al. Gaussian 09, revision A.02; Gaussian, Inc.: Wallingford, CT, 2009.

(19) Brasselet, S.; Zyss, J. *J. Opt. Soc. Am. B* **1998**, *15*, 257–288.

(20) Within the T convention, the $\overleftrightarrow{\beta}$ tensor is defined according to the expression $\vec{\mu} = \vec{\mu}_0 + \vec{\alpha} \cdot \vec{E} + 1/2 \overleftrightarrow{\beta} : \vec{E}\vec{E} + \dots$ where $\vec{\mu}_0$ is the permanent dipole moment, $\vec{\alpha}$ the polarizability tensor and \vec{E} the electric field.

(21) Heppke, G.; Parghi, D. D.; Sawade, H. *Liq. Cryst.* **2000**, *27*, 313–320.